Response of the Trilaminar Retinal Vessel Network to Intraocular Pressure Elevation in Rat Eyes

Da Zhao,[1] Zheng He,[1] Lin Wang,[2] Brad Fortune,[2] Jeremiah K.H. Lim,[1] Vickie H.Y. Wong,[1] Christine T.O. Nguyen,[1] and Bang V. Bui[1]

[1]Department of Optometry and Vision Sciences, University of Melbourne, Parkville, Victoria, Australia
[2]Devers Eye Institute, Legacy Research Institute, Portland, Oregon, United States

Correspondence: Bang V. Bui, Department of Optometry and Vision Sciences, University of Melbourne, 162 Monash Road, Parkville, Victoria 9010, Australia; bvb@unimelb.edu.au.

Received: April 27, 2019
Accepted: November 7, 2019
Published: February 7, 2020

Citation: Zhao D, He Z, Wang L, et al. Response of the trilaminar retinal vessel network to intraocular pressure elevation in rat eyes. *Invest Ophthalmol Vis Sci.* 2020;61(2):2. https://doi.org/10.1167/iovs.61.2.2

Purpose. The purpose of this study was to test the hypothesis that the superficial, intermediate, and deep retinal vascular plexus show different responses to intraocular pressure (IOP) elevation.

Methods. Anesthetized adult Long Evans rats (n = 14) were imaged using optical coherence tomography angiography (OCTA; Spectralis) at baseline (IOP 10 mm Hg) and in follow-up mode to examine the vasculature during IOP elevation (10 to 110 mm Hg, 10 mm Hg steps, each step 3 minutes). A 20° × 10° field was imaged. Vessel density within a 2D projection image was determined (%) for the superficial vascular complex (SVC), intermediate capillary plexus (ICP), and deep capillary plexus (DCP). Comparisons were made between layers using 2-way repeated measures ANOVA (layer versus IOP) following normalization to baseline (% relative to 10 mm Hg).

Results. The three vascular layers responded differently to IOP elevation. For IOPs between 40 and 60 mm Hg, DCP and ICP capillaries were significantly more resistant to IOP elevation than those in the SVC. When IOP was elevated above 70 mm Hg, all layers showed reduced vessel density. IOP induced change in SVC vessel density closely followed reductions in thickness of the inner retinal layers (nerve fiber, ganglion cell, and inner plexiform layer). This close relationship between reductions in tissue thickness and vessel density was less apparent for the ICP and DCP.

Conclusions. These data show that the intermediate and deep vascular plexus in the rat retina have a greater capacity for autoregulation against mild IOP elevation but are more affected at high IOP.

Keywords: angiography, intraocular pressure, trilaminar vascular network, autoregulation

The maintenance of an adequate oxygen and nutrient supply to the retina is critical for optimal retinal function. In species with vascularized retina, the inner and outer retina receives nutrition via the central retinal artery and the choroid, respectively.[1] Arising from the central retinal artery, the capillaries comprising the superficial vascular complex (SVC) lie within the ganglion cell layer and provide anastomoses to two deeper capillary beds located at the anterior and posterior aspects of the inner nuclear layer (INL). These two deeper capillary layers, known as the intermediate capillary plexus (ICP) and deep capillary plexus (DCP), serve the inner plexiform layer (IPL) and outer plexiform layer (OPL), respectively.[2] Metabolic exchange occurs within all plexi and is especially robust in the plexiform layers where oxygen extraction is maximal.[3]

The high energy demands of the retina along with its lack of energy stores makes it dependent on a robust capacity for the vasculature to maintain blood supply.[4] Although autonomic innervation of the choroidal vessels contributes to its regulatory control, the inner retina lacks such innervation and is entirely dependent on autoregulation mediated by the local release of vasoactive peptides.[5,6] Vasodilation and vasoconstriction occur in response to changes in metabolic demand associated with neurotransmission as well as to fluctuations in local pressure gradients that arise from changes in blood pressure or intraocular pressure (IOP).[7]

Laboratory studies demonstrate that autoregulation helps to maintain blood flow against elevation in IOP. Consistently, in response to a relatively low magnitude IOP elevation (10-40 mm Hg), vasodilation occurs to prevent a drop in blood flow.[8,9] When IOP elevation reaches 60 to 70 mm Hg, autoregulation mechanisms are overwhelmed resulting in forceful compression of inner retinal vessels and attenuation of blood flow.[10] Although many studies have documented autoregulation-induced changes in the larger surface vessels, few have considered the smaller vessels. Moreover, approaches, such as video-angiography,[11] Doppler flowmetry,[10] and laser speckle flowgraphy,[12] lack the depth (axial) and lateral (transverse) resolution to differentiate changes within the three retinal capillary plexi.

The advent of optical coherence tomography angiography (OCTA) has facilitated clinical and laboratory studies of the normal trilaminar vasculature[2,13,14] and the impact of a range of retinal conditions on the vasculature.[15–17] A number

of investigations have used OCTA to investigate how the retinal and optic nerve vasculature responds to acute IOP elevations.[18] Zhang et al.[19] showed in human subjects, that IOP elevation of 10 to 15 mm Hg above baseline induced via a dark-room prone test did not affect OCTA vessel density. In laboratory studies, experiments in rats showed that vessel density was unchanged until IOP was elevated to 40 to 50 mm Hg.[20,21] Patel et al.[22] showed that IOP elevation to 60 mm Hg significantly reduced peripapillary vessel density in non-human primates. Zhi et al.[20] also showed that different vascular beds (retinal, choroidal, and optic nerve vessels) may respond differently to acute IOP elevation.

In addition to differences between particular regions of the retina, there may also be differences in autoregulation between the various retinal vessel plexi. Using OCTA, Son et al.[23] show that, in response to flickering light, the ICP and DCP showed a greater hemodynamic response compared with the SVC. Similarly, Kornfield and Newman[24] showed that flickering light stimulation in rat retina evoked greater vasodilation in the intermediate capillary layer compared with superficial and deep capillary layers. Data reported by Augustin et al.[25] suggest that at high IOP, above 65 mm Hg, deeper retinal vessels in the rat retina were more attenuated than the superficial vessels. Therefore, it remains unclear whether differences exist between the way the various vascular layers autoregulate against IOP elevation. In this study, we use OCTA to quantify vessel density in the superficial, intermediate, and deep vessel plexi across a wide range of IOP levels. We also compared changes in vessel density to changes in retinal structure.

Materials and Methods

Animals

All procedures were approved by the Howard Florey Animal Ethics Committee (13-044-UM) and performed according to the guidelines outlined by the National Health and Medical Research Council of Australia. Experiments were undertaken in 14 adult Long Evans rats (Animal Resource Centre, Caning Vale, WA, Australia). Rats were housed within the Melbourne Brain Centre animal facility at a temperature of 20°C, a 12-hour light/dark cycle (below 50 lux on at 7AM, off at 7PM) with access to chow (Barastoc, Ridley, Melbourne, VIC, Australia) and water ad libitum.

All procedures were conducted while the subjects were under general anesthesia using a mixture of ketamine (60 mg/kg) and xylazine (5 mg/kg; Troy Laboratories, Smithfield, NSW, Australia) delivered via an intraperitoneal injection. Adequate depth of anesthesia was monitored by absence of the paw pinch reflex. A topical anesthetic (Ophthetic 5 mg/mL; Allergan, Gordon, NSW, Australia) and mydriatic (Mydriacyl 5 mg/mL, Alcon laboratories, Frenchs Forest, NSW, Australia) were also applied to each eye before imaging.

Blood Pressure Monitoring

Blood pressure was monitored via an indwelling cannula in the left femoral artery, as has been previously described.[10] Briefly, a heparinized polyethylene cannula (inner and outer diameter 0.28 and 0.61 mm, respectively) was inserted 3 cm proximally into the left femoral artery. The exterior end of the cannula was connected to a pressure transducer (Transpac; Abbott Critical Care Systems, Sligo, IRE) to give direct and continuous blood pressure monitoring (ADInstruments Pty Ltd, Bella Vista, NSW, Australia). Following surgery for blood pressure assessment, animals were placed on a heated platform to maintain core temperature at 37°C, and had one randomly chosen eye cannulated for IOP manipulation. Average blood pressure for the group was 113 mm Hg (n = 14, SD ± 10 mm Hg).

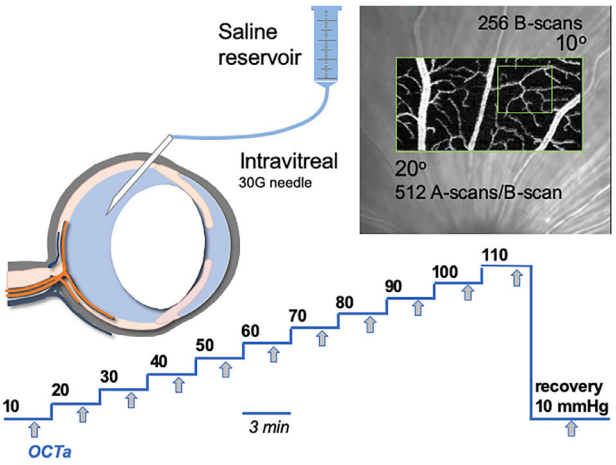

Figure 1. Experimental protocol. Anesthetized rats underwent vitreal chamber cannulation using a 30G needle. OCTA volumes were collected at IOP levels from baseline (10 mm Hg) to 110 mm Hg, in 10 mm Hg steps. At each step, imaging began 2 minutes following the onset of IOP elevation. Volumes were 10 (vertical) by 20 (horizontal) degrees, consisting of 256 B-scans, each made up of 512 A-scans and 5 scan repeats. The volume collected at baseline was set as the reference and subsequent volumes were collected in follow-up mode.

Intraocular Pressure Manipulation

A gradient of IOP levels was achieved via stepwise IOP elevation from 10 to 110 mm Hg via a vitreous chamber cannula (Fig. 1). As previously described,[26] the eye was cannulated with a 30 G needle (Fig. 1) connected via polyethylene tubing (0.8 mm outer and 0.4 mm inner diameters; Unomedical, Sydney, NSW, Australia) to a fluid reservoir (60 mL syringe) containing Hanks balanced salt solution (Merck, Darmstadt, Germany). The target IOP was achieved by placing the reservoir at heights precalibrated to a manometer (Livingstone, Sydney, NSW, Australia). It is important to ensure that needles do not become blocked. All needles were pretested to rule out blockage. During insertion the pressure head was set to 20 mm Hg and flow of fluid was confirmed. Pressure was returned to 10 mm Hg for baseline imaging. As pressure increased above 30 mm Hg, greater pupil dilation and increased venous pulsatility confirmed needle patency. At the end of experimentation, the pressure was returned to 20 mm Hg and fluid flow was once again confirmed. Leakage can occasionally occur, as would be evident by fluid pooling outside the eye, however, this did not occur in the current study.

Experimental Protocol

Following vitreous chamber cannulation, IOP was set to 10 mm Hg as baseline. A baseline OCTA volume was recorded using a spectral domain OCT/OCTA system

Investigative Ophthalmology & Visual Science

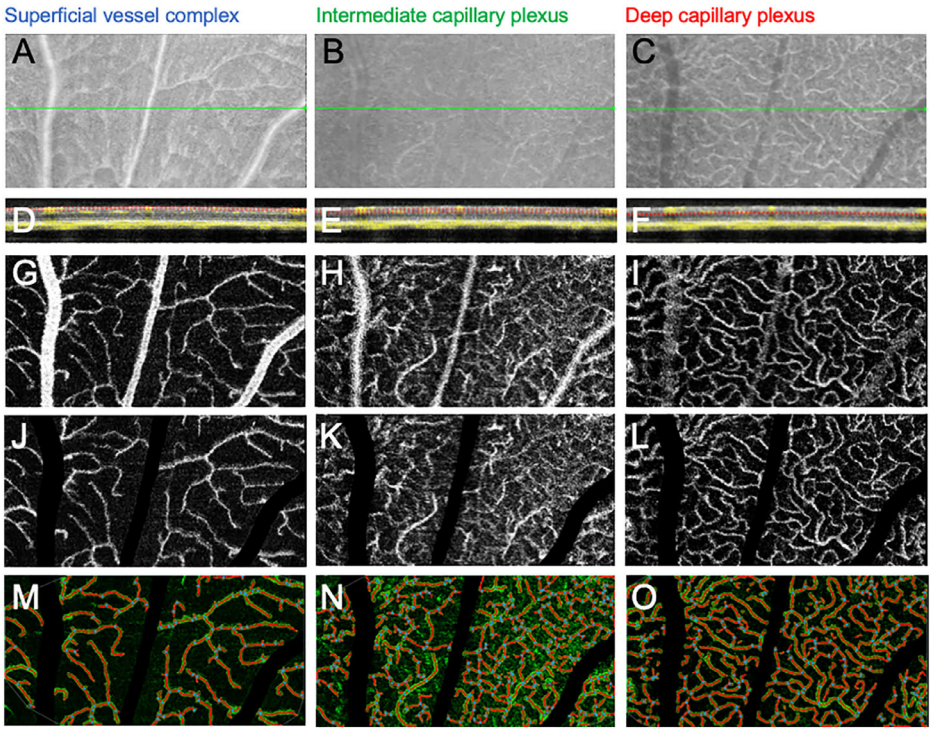

Figure 2. Segmentation of vessel layers. (**A–C**) The upper row of images shows the en face infrared projection of the tissue slab containing the specific vessel layer as defined by the structural OCT (**D–F**). (**G–I**) The third row shows en face angiography projection for the SVC (**G**), ICP (**H**) and DCP (**I**). (**J-L**) Large vessels were masked using ImageJ prior to analysis. (**M-O**) Vessel layers were analyzed using AngioTool to return the % area within the region of interested occupied by vessels (highlighted in green, vessel center shown by red traces).

(Spectralis OCT2; Heidelberg Engineering, Heidelberg, Germany) with the aid of a rodent objective lens attachment (25D, Heidelberg Engineering). Images were acquired with a volume scan pattern of 20° × 10° (5.4 × 2.7 mm) starting at one-disc diameter from the optic nerve head (see Fig. 1). Each volume consisted of 256 vertical B-scans (5 repeats) each consisting of 512 A-scans.

For each eye, the baseline volume was processed and set as the reference volume. IOP was then elevated in steps of 10 mm Hg up to 110 mm Hg, each step lasting 3 minutes. At the two-minute mark into each IOP level, the OCTA volume was recorded. After the last step (110 mm Hg) IOP was gradually returned (approximately 10 seconds) to 10 mm Hg by lowering the fluid reservoir back to baseline. A final OCTA recording was obtained 2 minutes after IOP normalization to baseline to assess recovery of the vasculature.

Image Processing and Analysis

Similar to the approach of Smith et al.,[15] segmentation of the individual retinal layers (retinal nerve fiber layer [RNFL], ganglion cell layer [GCL], IPL, INL, OPL, outer nuclear layer [ONL], and total retinal thickness [TRT]) and three vascular plexi (SVC, ICP, and DCP) was conducted using the automated software in-built into the imaging platform (Heidelberg Engineering). Each volume was checked for segmentation errors. Layer thicknesses were measured across the structural volume. The automated algorithm, although designed for human retinae, is able to reliably segment retinal layers in OCTA images collected from rodent eyes.[27] In terms of the vascular plexi, the three layers are segmented based on the structural information. Consistent with Campbell et al.[2] the SVC reflects the presence of patent blood vessels in the inner retina (RNFL, GCL, and midway through the IPL to incorporate the vascular bed at the GCL-IPL interface). The ICP reflects the intermediate vascular bed, which lies between the IPL-INL interface (quantified as the detectable vasculature present from the middle of the IPL to the middle of the INL layers). Finally, the DCP lies between the INL-OPL interface and is, thus, segmented midway between the INL and OPL. An example of the structural B-scans and the segmentation that defines the vascular layers is shown in Figures 2D through 2F, along with the en face projection of these volumes in Figures 2A through 2C. OCTA images were exported as tiff images, as shown in Figures 2G through 2I.

In ImageJ, tiff images were combined into a stack. Using the baseline SVC, a mask was generated to remove the larger vessels from all images. These images were subsequently analyzed using AngioTool[28] to return the vessel area as a proportion of the region of interest detectable by OCTA. AngioTool uses a thresholding algorithm to create a binarized image. It then automatically segments the vessels to identify the total vessel area.[28] All vessel profiles that had been skeletonized (Figs. 2J through 2L) are identifiable in green, with their centers shown by the red traces, and each branch point indicated by a blue dot (Figs. 2M–2O). Comparison shows that AngioTool returns a robust estimate of the vessel area as compared against analyses of images using a thresholding and binarizing algorithm in ImageJ (Supplementary Fig. S1).

In addition to the 20° × 10° region of interest, a 5° × 5° region between the major vessels was analyzed to ensure that projection artifacts from the major vessels was minimized. The latter analysis also facilitated comparison of vessels of similar diameter across the three layers. For each

Investigative Ophthalmology & Visual Science

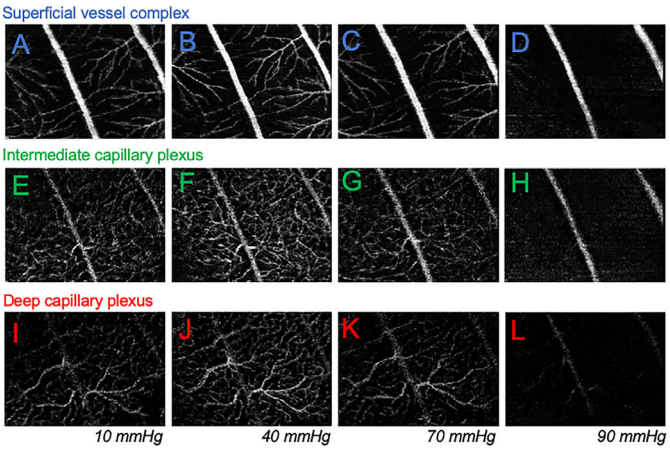

Figure 3. Effect of IOP elevation on vessel layers in a representative rat eye. (**A–D**) The SVC for the same eye when IOP was at 20, 40, 70, and 90 mm Hg. (**E-H**) Effect of IOP elevation on the ICP for the same eye. (**I-L**) Effect of IOP elevation on the DCP for the same eye.

IOP step, the vessel area was expressed as a percentage change relative to baseline.

Statistical Analysis

Grouped data are shown as the average ± standard error of the mean (SEM). Statistical analysis of all data was conducted using Prism 7 (GraphPad Software Inc., San Diego, CA, USA). For each individual layer, the effect of IOP on the retinal structure or vasculature was analyzed using a 1-way RM-ANOVA (with Greenhouse-Geisser correction) and a post hoc Dunnett's test was used to compare changes against baseline (IOP at 10 mm Hg). To compare responses between multiple retinal layers, a 2-way RM-ANOVA and a Sidak post hoc test was used to compare changes in structure and vasculature across IOP levels.

Results

Figure 3 shows a representative example of how the various vascular layers were affected by IOP elevation. Compared with baseline IOP at 10 mm Hg (Figs. 3A, 3E, 3I), at 40 mm Hg more vessels were visible, particularly the intermediate (Fig. 3F) and deep plexus (Fig. 3J). At 70 mm Hg, there was evidence of attenuation of smaller vessels in all three layers (Figs. 3C, 3G, 3K), whereas larger vessel in the SVC seemed to be wider (Fig. 3C). With IOP elevated to 90 mm Hg, the smaller vessels were no longer detectable, the largest vessels in the SVC could still be seen (Fig. 3D). IOP induced to vessels changes were associated with alterations to the appearance of the fundus, as shown in Supplementary Figure S2. With gradually higher levels of IOP elevation, the surface of the rat optic nerve shows posterior deformation. For IOPs of 60 mm Hg or higher, the scleral canal becoming more visible and the larger vessels were less visible around the optic nerve.

Figure 4 summarizes the vascular response of the group to IOP elevation, both as raw vessel density (Figs. 4A, 4B) and expressed relative to baseline IOP (Figs. 4C, 4D). Vessels were analyzed over the entire 20° × 10° region of interest or in a subregion (5° × 5°) containing only small vessels to minimize projection artifacts produced by larger vessels.

At baseline, there were significant differences between all vascular layers (Fig. 4A; $F_{2,13} = 23.2$, $P < 0.001$; all pairwise $P < 0.05$). The highest vessel density was found in the DCP (30.5 ± 1.7%), followed by the SVC (27.0 ± 1.1%), with the lowest density found in the ICP (24.4 ± 1.5%). A similar pattern emerged when a smaller region of interest that excluded the large vessels was analyzed (Fig. 4B; DCP 27.4 ± 2.1%; SVC 22.7 ± 2.5%; ICP 17.5 ± 1.9%; $F_{2,13} = 16.9$, $P < 0.001$), with post hoc comparison showing that capillary density was similar in the SVC and DCP ($P > 0.05$) and both were higher than the ICP ($P < 0.05$).

Analysis of raw vessel density showed that IOP elevation significantly affected the SVC (Fig. 4A, 1-way RM-ANOVA, $F_{13,130} = 52.6$; $P < 0.001$), with post hoc comparison identifying significant attenuation for IOPs above 80 mm Hg. Significant IOP effects on ICP ($F_{11,130} = 35.4$; $P < 0.001$) and DCP vessel density ($F_{11,120} = 48.9$, $P < 0.001$) were also observed, with post hoc analysis highlighting reductions from baseline for IOPs above 80 mm Hg. A similar pattern was observed when a subregion of interest excluding the larger vessels was analyzed (Fig. 4B), with the exception that post hoc analysis ($F_{11,130} = 27.1$, $P < 0.001$) revealed that the smaller vessels in the SVC were attenuated at a lower IOP level of 60 mm Hg. For the DCP and ICP, significant attenuation was found when IOP exceeded 80 mm Hg 2 minutes following restoration of IOP back to a baseline of 10 mm Hg vessel density on all layers had returned to normal (Fig. 4; all $P > 0.05$).

Comparisons Between Layers

Comparisons between layers were undertaken on data normalized to baseline (Figs. 4C, 4D). There was no significant interaction between the SVC and ICP (Fig. 4C; 2-way RM-ANOVA, IOP × layer $F_{9,117} = 1.28$, $P = 0.25$), however, there was a significant difference between layers (Layer $F_{1,13} = 6.5$, $P = 0.02$). Post hoc comparison showed vessel density SVC was more attenuated by IOP compared with the ICP at 60 and 70 mm Hg. In contrast, comparison between the SVC and DCP revealed a significant interaction between layer and IOP (IOP × layer $F_{9,117} = 3.9$, $P = 0.0002$), with the SVC significantly more affected than the DCP at 60 and 70 mm Hg. However, the SVC was less affected than the DCP at 90 mm Hg. Similarly, a significant interaction was also

Investigative Ophthalmology & Visual Science

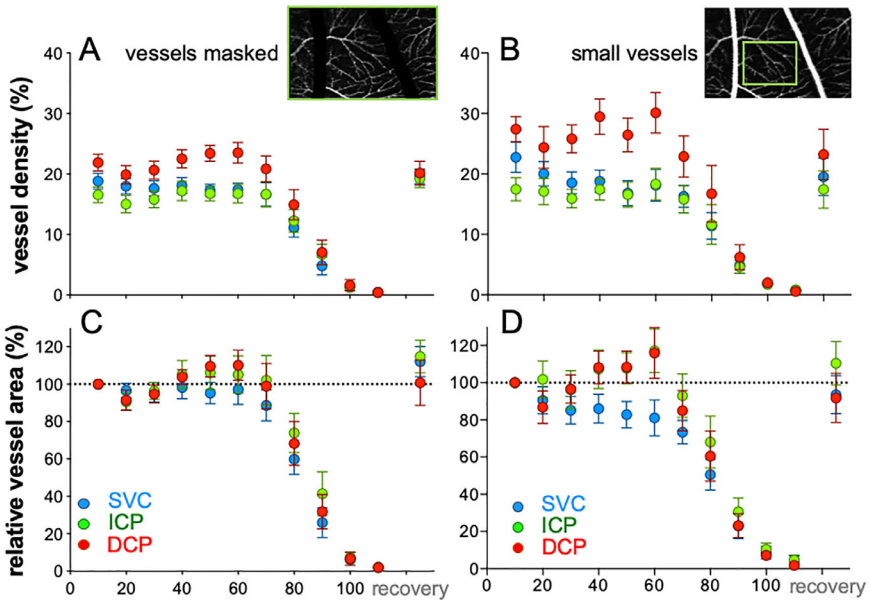

Figure 4. IOP elevation affects the superficial vessel differently to the deeper layers. (**A**) Group average (±SEM, n = 14) relative vessel area for the entire region of interest (20 × 10°) analyzed after masking the large vessels, plotted as function of IOP for the SVC, ICP, and DCP. (**B**) Relative vessel area for 5 × 5° regions of interest that do not contain large vessels to minimize confound associated with projection artifacts.

observed between the ICP and DCP (IOP × layer $F_{9,117} = 4.3$, $P < 0.001$), with post hoc analysis identifying that the DCP was more affected than the ICP at high IOPs (90 and 100 mm Hg).

Figure 4D compares the effect of IOP elevation on small vessels in the three vascular layers. The difference between the superficial and the two deeper layers was more apparent. There was a significant interaction between SVC and the ICP ($F_{9,117} = 39.6$, $P < 0.001$), as well as between SVC and DCP as a function of IOP ($F_{9,117} = 40.5$, $P < 0.001$). In both cases, post hoc analysis showed that the SVC was more attenuated at 40, 50, and 60 mm Hg compared with the deeper layers.

The three vascular layers were also considered together by summing the vessel area at baseline such that this was 100% (Supplementary Fig. S2) and expressing all areas relative to 100%. This shows that although there was an increase in vessel area in the DCP (Supplementary Fig. S3A), overall there was no change for all three layers combined for IOPs below 80 mm Hg (Supplementary Fig. S3B).

Relationship Between Vessel Density and Tissue Thickness

Figure 5 summarizes the effect of IOP elevation on the thickness of the various retinal layers and compares these IOP effects to those on the vasculature. Total retinal thickness (Fig. 5A) was slightly but significantly reduced by IOP elevation (1-way R-ANOVA, $F_{13,130} = 21.0$, $P < 0.001$) in a linear manner, with significant post hoc differences detected for IOPs above 30 mm Hg. Maximal retinal thickness reduction of 4.5 ± 3.4% was observed at 100 mm Hg (Fig. 5D).

Figure 5B shows that the thickness of inner retinal layers (RNFL $F_{13,130} = 24.7$, $P < 0.001$; IPL $F_{13,130} = 19.4$, $P = 0.001$) was slightly reduced by IOP elevation between IOPs of 20 and 80 mm Hg, whereas for IOPs between 90 and 110 mm Hg there were more dramatic effects. Post hoc analysis identified significant reduction from baseline for IOPs above 70 mm Hg for the RNFL. For the IPL, significant post hoc reductions from baselines were returned for 40 and 60 mm Hg as well as all IOPs above 70 mm Hg. At the highest IOP of 110 mm Hg, RNFL and IPL were compressed by 43.0 ± 13.9% and 32.6 ± 12.7%, respectively. Comparison between the RNFL and IPL (Fig. 5E) revealed that the RNFL was significantly more compressed by IOP elevation (2-way RM-ANOVA, IOP × layer $F_{9,117} = 7.4$, $P < 0.001$); particularly for IOP above 70 mm Hg (post hoc, $P < 0.05$).

Unlike the inner retinal layers, which showed significant thickness reduction, the INL was not significantly affected by IOP elevation (Fig. 5C; $F_{13,130} = 1.1$, $P = 0.35$) and the OPL showed significant thickening at the highest pressure (Fig. 5C; $F_{13,130} = 3.2$, $P = 0.03$). Comparison between the INL and the OPL (Fig. 5F) showed a significant interaction between layer and IOP (2-way RM-ANOVA, $F_{9,117} = 5.6$, $P < 0.001$), with post hoc differences at 100 and 100 mm Hg (post hoc, $P < 0.05$). The INL was maximally reduced by 3.8 ± 9.2%, whereas the OPL seemed to swell by 5.3 ± 9.4% (Fig. 5F).

Figures 5G, 5H, and 5I overlay relative vessel density (right hand axes labels) for each of the three vascular layers along with the respective structural layers where these vascular beds reside. Note that the range for the relative thickness axes for Figures 5G and 5H have been selected such that the relative thickness at 110 mm Hg align with 0% vessel density (Fig. 5I range has been set as per Fig. 5H for comparison). This approach to visualization makes it apparent that reduction in the RNFL/GCL/IPL thickness closely follows the attenuation of the SVC (Fig. 5G). Figure 5H shows that for IOP above 60 mm Hg, reduction of the IPL combined with the INL thickness parallels the attenuation of the ICP, however, at lower pressure (range from 20–60 mm Hg), despite apparent tissue layer thinning, the vessel density was not reduced. IOP effects on INL and OPL thickness did not follow change in DCP vessel density (Fig. 5I).

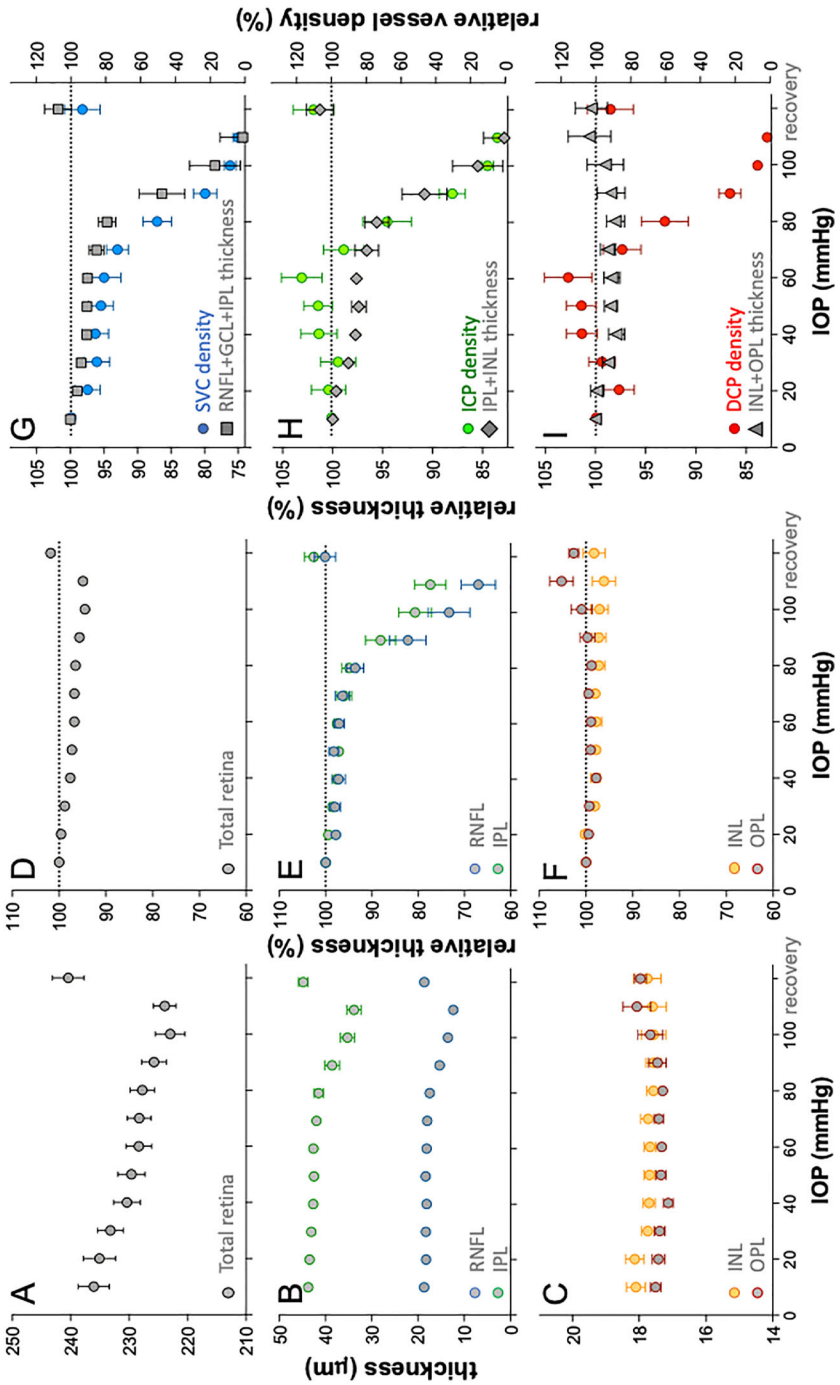

Figure 5. Effect of IOP elevation on retinal thickness and their relationship to vessel area. (**A**) Average (±SEM, n = 14) total retinal thickness plotted as function of IOP. (**B**) Average RNFL IPL thickness versus IOP. (**C**) Average INL and OPL thickness versus IOP. (**D**) Total retinal thickness relative to baseline (%) plotted as function of IOP. (**E**) Relative (%) RNFL and IPL thickness versus IOP. (**F**) Relative (%) INL and OPL thickness versus IOP. (**G**) Relative SVC vessel density overlaid with relative thickness of combined RNFL, GCL, and IPL. (**H**) Relative ICP vessel density over and laid with relative thickness of combined IPL and INL. (**I**) Relative deep capillary plexus (DCP) vessel density overlaid with relative thickness of combined INL and OPL.

Discussion

We show that acute, controlled elevation of IOP significantly affected vessel density and retinal thickness as measured using OCT/OCTA. Vessel density did not decline in a linear fashion but followed a sigmoidal function. Similar patterns of vascular responses to IOP elevation have been noted in other studies of the rat retina, including those using other measures of perfusion, such as Doppler flowmetry.[10,29] In particular, studies using OCT microangiography have shown that retinal blood flow declines at IOP levels of 40 mm Hg or higher.[20,21] Our observations for the small vessels in the SVC (Fig. 4D) showed significant reduction in vessel density for IOPs >60 mm Hg. This is consistent with previous work in rats.[21,30]

When our analysis included the larger vessels (Figs. 4A, 4C) the SVC did not show significant attenuation until IOP reach high levels (>80 mm Hg). This would suggest that the caliber of larger vessels better resists IOP elevation.

Our data show that not all retinal vessel layers were affected by IOP elevation in the same way. In particular, we show that when measurements are isolated to the small vessels, moderate IOP elevation, to a level between 20 and 60 mm Hg, affected the SVC more than the ICP and DCP (Fig. 4D). At very high IOP levels (between 80 and 110 mm Hg), vessels within all three layers were attenuated. Other studies have also shown that different locations in the rodent eye are affected differently by IOP elevation. Zhi et al.[20] reported that choroidal and optic nerve head perfusions measured using OCT microangiography were more resistant to IOP elevation than retinal perfusion. Augustin et al.[25] used OCT to measure vessel pulsatility as an index of blood flow (or flux) and studied the effect of IOP elevation on the superficial retinal plexus and the deeper retinal capillary plexus at the rat optic nerve head. They showed that significant attenuation of flux occurred at a high IOP of 95 mm Hg for the deeper capillary plexus compared with 85 mm Hg for the superficial vessels. However, the small sample size of their study (n = 5) made differences between layers difficult to detect. In our study, when the IOP was raised between 20 and 60 mm Hg there was a reduction in SVC vessel density, whereas there was little change in the ICP or DCP (Fig. 4D).

It is worth noting that IOP elevation can increase vessel pulsatility, potentially manifesting as the appearance of a thicker blood column on OCTA.[31] However, one might expect such flow artifacts to affect the entire vascular bed and produce apparent increases in all vascular layers. That we observed a reduction in small vessel density in the SVC but not the ICP and DCP might argue against this possibility. Zhi et al.[20] raised the possibility that vessels in deeper structures can increase in visibility if blood flow in overlying layers decreases, thus there is less attenuation of the light by these overlying vessels. If this were the case, one might expect that as flow decreases in the SVC, the ICP and the DCP would show a greater apparent increase. That the middle (ICP) and deepest (DCP) vascular layers show the same pattern of change with IOP elevation argues that this alone is an unlikely explanation for our findings.

Leahy et al.[13] using mapping of rat retinal blood vessels suggest that the different vascular layers in the rat retina show varying degrees of interconnectedness. The density of vessels connecting the ICP and DCP was the highest, some three times denser that the connection between the SVC and ICP. Additionally, there are a number of connections directly from the SVC down to the DCP, albeit much fewer than between adjacent layers. Therefore, IOP elevation can push blood from the superficial layer down to the DCP either via the ICP or directly.

IOP-induced changes to blood flow through the interconnecting vessels could contribute to our observed increased in vessel area in the ICP and DCP at moderate IOP levels. Our analysis approach is unable to differentiate between presumed vessel dilation and increased contributions from interconnecting vessels. The type of 3D mapping analysis used by Leahy et al.[13] would be highly informative applied to IOP-induced vascular changes.

Reduced tissue thickness of the RNFL and IPL followed a similar qualitative pattern with IOP elevation to SVC vessel density: there was slight reduction with mild to moderate IOP elevation (to IOP levels between 10 and 70 mm Hg), followed by greater reduction for IOPs of 80 mm Hg or higher (Figs. 5B, 5G). This close relationship was less apparent for the ICP (Fig. 5H) and DCP (Fig. 5I). One possibility is that increased venous pressure associated with IOP elevation[32] leads to blood shunting into the deeper vessel layers. Shunting of blood from capillaries (<8 µm) into slightly larger vessels (8–15 µm) has been observed in the cerebral cortex of rats when the tissue pressure (intracranial pressure) was increased by 20 mm Hg.[33]

Another possible mechanism is that vessels in the SVC show less capacity to resist IOP elevation than the ICP and DCP (Fig. 4D). Data from ex vivo and in vivo experiments of the rat retinal vasculature shows that in response to increased demand for blood induced by flickering light (functional hyperemia), vessels in the intermediate layer showed greater vasodilation compared with capillaries in the superficial and deep vessel plexi.[24] These mechanisms require further investigation.

It is important to note that the binarized OCTA images analyzed in this study returns a measure of vessel caliber and not flow per se. Therefore, the extent of "autoregulation" examined is limited to only that which manifests as a change in caliber. An important technical limitation of studying different vascular plexi using OCTA is projection artifacts. Although we used a number of strategies, including the manufacturer's projection artifact rejection algorithm, masking of larger vessels and analyzing areas away from the larger vessels, projection artifacts are still to be considered a problem in quantitative comparison between layers. It is important to note that OCT shadowing artifacts and low OCT reflectance can exaggerate low or nonperfusion.

This study has been limited to acute short-term increase in IOP used to probe the vasculature of the healthy, rod-dominated retina. As we had not undertaken any post-mortem analysis, it is not clear if the IOP protocol used in this study has any long-term impact on retinal or vascular structure. Therefore, studying the effect of acute IOP elevation as well as the effect of chronic IOP elevation to magnitudes that are more relevant to the development of inner retinal injury will provide deeper insights into how the various retinal layers are affected in glaucoma.

In conclusion, we find that with mild IOP elevation small vessels in the superficial vessel complex were more affected than those in the intermediate and deep capillary plexi in rat retina. Attenuation of blood flow in the SVC was closely associated with reduced tissue thickness of the RNFL and GCL, whereas changes in the intermediate and deep capillary plexi could not fully account for changes in tissue thickness. That inner retinal layers and vessels in the SVC were more

Investigative Ophthalmology & Visual Science

affected by IOP elevation has implications for understanding how IOP elevation might preferentially impact nutrient supply to the nerve fiber layer and ganglion cells.

Acknowledgments

Supported by the Australian Research Council Future Fellowship, R01-EY019939; Legacy Good Samaritan Foundation.

Disclosure: **D. Zhao,** None; **Z. He,** None; **L. Wang,** None; **B. Fortune,** None; **J.K.H. Lim,** None; **V.H.Y. Wong,** None; **C.T.O. Nguyen,** None; **B.V. Bui,** None

References

1. Bill A, Sperber GO. Aspects of oxygen and glucose consumption in the retina: effects of high intraocular pressure and light. *Graefes Arch Clin Exp Ophthalmol*. 1990;228:124–127.
2. Campbell JP, Zhang M, Hwang TS, et al. Detailed vascular anatomy of the human retina by projection-resolved optical coherence tomography angiography. *Sci Rep*. 2017;7:42201.
3. Yu DY, Cringle SJ. Oxygen distribution and consumption within the retina in vascularised and avascular retinas and in animal models of retinal disease. *Prog Retin Eye Res*. 2001;20:175–208.
4. Riva CE, Sinclair SH, Grunwald JE. Autoregulation of retinal circulation in response to decrease of perfusion pressure. *Invest Ophthalmol Vis Sci*. 1981;21:34–38.
5. Hayreh SS. Blood flow in the optic nerve head and factors that may influence it. *Prog Retin Eye Res*. 2001;20:595–624.
6. Pournaras CJ, Riva CE, Bresson-Dumont H, De Gottrau P, Bechetoille A. Regulation of optic nerve head blood flow in normal tension glaucoma patients. *Eur J Ophthalmol*. 2004;14:226–235.
7. Delaey C, Van De Voorde J. Regulatory mechanisms in the retinal and choroidal circulation. *Ophthalmic Res*. 2000;32:249–256.
8. Li H, Bui BV, Cull G, Wang F, Wang L. Glial cell contribution to basal vessel diameter and pressure-initiated vascular responses in rat retina. *Invest Ophthalmol Vis Sci*. 2017;58:1–8.
9. He Z, Lim JK, Nguyen CT, Vingrys AJ, Bui BV. Coupling blood flow and neural function in the retina: a model for homeostatic responses to ocular perfusion pressure challenge. *Physiological Reports*. 2013;1:e00055.
10. He Z, Nguyen CT, Armitage JA, Vingrys AJ, Bui BV. Blood pressure modifies retinal susceptibility to intraocular pressure elevation. *PLoS One*. 2012;7:e31104.
11. Nguyen TT, Kreis AJ, Kawasaki R, et al. Reproducibility of the retinal vascular response to flicker light in Asians. *Curr Eye Res*. 2009;34:1082–1088.
12. Wang L, Cull GA, Fortune B. Optic nerve head blood flow response to reduced ocular perfusion pressure by alteration of either the blood pressure or intraocular pressure. *Curr Eye Res*. 2015;40:359–367.
13. Leahy C, Radhakrishnan H, Weiner G, Goldberg JL, Srinivasan VJ. Mapping the 3D connectivity of the rat inner retinal vascular network using OCT angiography. *Invest Ophthalmol Vis Sci*. 2015;56:5785–5793.
14. Tan B, MacLellan B, Mason E, Bizheva KK. The effect of acutely elevated intraocular pressure on the functional and blood flow responses of the rat retina to flicker stimulation. *Invest Ophthalmol Vis Sci*. 2017;58:5532–5540.
15. Smith CA, Hooper ML, Chauhan BC. Optical coherence tomography angiography in mice: quantitative analysis after experimental models of retinal damage. *Invest Ophthalmol Vis Sci*. 2019;60:1556–1565.
16. Shah RS, Soetikno BT, Yi J, et al. Visible-light optical coherence tomography angiography for monitoring laser-induced choroidal neovascularization in mice. *Invest Ophthalmol Vis Sci*. 2016;57:OCT86–95.
17. Park JR, Choi W, Hong HK, et al. Imaging laser-induced choroidal neovascularization in the rodent retina using optical coherence tomography angiography. *Invest Ophthalmol Vis Sci*. 2016;57:OCT331–340.
18. Kashani AH, Chen CL, Gahm JK, et al. Optical coherence tomography angiography: a comprehensive review of current methods and clinical applications. *Prog Retin Eye Res*. 2017;60:66–100.
19. Zhang Q, Jonas JB, Wang Q, et al. Optical coherence tomography angiography vessel density changes after acute intraocular pressure elevation. *Sci Rep*. 2018;8:6024.
20. Zhi Z, Cepurna WO, Johnson EC, Morrison JC, Wang RK. Impact of intraocular pressure on changes of blood flow in the retina, choroid, and optic nerve head in rats investigated by optical microangiography. *Biomedical Optics Express*. 2012;3:2220–2233.
21. Jiang X, Johnson E, Cepurna W, et al. The effect of age on the response of retinal capillary filling to changes in intraocular pressure measured by optical coherence tomography angiography. *Microvasc Res*. 2018;115:12–19.
22. Patel N, McAllister F, Pardon L, Harwerth R. The effects of graded intraocular pressure challenge on the optic nerve head. *Exp Eye Res*. 2018;169:79–90.
23. Son T, Wang B, Thapa D, et al. Optical coherence tomography angiography of stimulus evoked hemodynamic responses in individual retinal layers. *Biomedical Optics Express*. 2016;7:3151–3162.
24. Kornfield TE, Newman EA. Regulation of blood flow in the retinal trilaminar vascular network. *J Neurosci*. 2014;34:11504–11513.
25. Augustin M, Fialova S, Fischak C, Schmetterer L, Hitzenberger CK, Baumann B. Ocular fundus pulsations within the posterior rat eye: chorioscleral motion and response to elevated intraocular pressure. *Sci Rep*. 2017;7:8780.
26. Zhao D, He Z, Vingrys AJ, Bui BV, Nguyen CT. The effect of intraocular and intracranial pressure on retinal structure and function in rats. *Physiological Reports*. 2015;3:e12507.
27. Dysli C, Enzmann V, Sznitman R, Zinkernagel MS. Quantitative analysis of mouse retinal layers using automated segmentation of spectral domain optical coherence tomography images. *Transl Vis Sci Technol*. 2015;4:9.
28. Zudaire E, Gambardella L, Kurcz C, Vermeren S. A computational tool for quantitative analysis of vascular networks. *PLoS One*. 2011;6:e27385.
29. Lim JK, Nguyen CT, He Z, Vingrys AJ, Bui BV. The effect of ageing on ocular blood flow, oxygen tension and retinal function during and after intraocular pressure elevation. *PLoS One*. 2014;9:e98393.
30. Zhi Z, Cepurna W, Johnson E, Jayaram H, Morrison J, Wang RK. Evaluation of the effect of elevated intraocular pressure and reduced ocular perfusion pressure on retinal capillary bed filling and total retinal blood flow in rats by OMAG/OCT. *Microvasc Res*. 2015;101:86–95.
31. Spaide RF, Fujimoto JG, Waheed NK. Image artifacts in optical coherence tomography angiography. *Retina*. 2015;35:2163–2180.
32. Morgan WH, Yu DY, Cooper RL, Alder VA, Cringle SJ, Constable IJ. Retinal artery and vein pressures in the dog and their relationship to aortic, intraocular, and cerebrospinal fluid pressures. *Microvasc Res*. 1997;53:211–221.
33. Bragin DE, Bush RC, Muller WS, Nemoto EM. High intracranial pressure effects on cerebral cortical microvascular flow in rats. *J Neurotrauma*. 2011;28:775–785.